Electronic Supplementary Information

Molecular Recognition of Organophosphorus Compounds in Water and Inhibition of Their Toxicity to Acetylcholinesterase

Wei-Er Liu,[ab] Zhao Chen,[b] Liu-Pan Yang,[b] Ho Yu Au-Yeung,*[a] and Wei Jiang *[b]

[a] *Department of Chemistry, The University of Hong Kong, Hong Kong, China. E-mail: hoyuay@hku.hk*

[b] *Shenzhen Grubbs Institute and Department of Chemistry, Southern University of Science and Technology, Shenzhen, 518055, China. E-mail: jiangw@sustech.edu.cn*

Table of Contents

1. Experimental Section

1.1 General. All the reagents involved in this research were commercially available and used without further purification unless otherwise noted. Solvents were either employed as purchased or dried prior to use by standard laboratory procedures. ^{1}H NMR and ^{31}P NMR spectra were recorded on Bruker Avance-400M or 500M NMR spectrometers. All chemical shifts are reported in *ppm* with methylsulfonic acid as the internal standard. Fluorescence spectra (FL) were obtained on a Shimadzu RF-5301pc spectrometer. UV-vis absorption spectra were obtained on a Hitachi U-2600 UV-vis spectrophotometer. Molecular simulations were performed at the Semi-Empirical PM6 level of theory by using Spartan'14 (Wavefunction, Inc.). The synthesis of **1a** and **1b** has been reported.[1]

1.2 Isothermal titration calorimetry, ITC. Titration experiments were carried out in deionized water at 25 °C on a VP-ITC instrument. In a typical experiment, a 1.4338 mL solution of **1a** was placed in the sample cell at a concentration of 1.0×10^{-4} M, and 292 μL of a solution of **7** (3.0×10^{-3} M) was in the injection syringe. The titrations were consisted of a 2 μL injection and followed 28 consecutive injections of 10 μL each with a 210 s interval between injections. Heats of dilution, measured by titration of **7** into the sample cell with blank solvent, were subtracted from each data set. All solutions were degassed prior to titration. The data were analysed using the instrumental internal software package and fitted by "one binding site" model. Errors are smaller than ±10%.

1 G. B. Huang, S. H. Wang, H. Ke, L. P. Yang and W. Jiang, *J. Am. Chem. Soc.*, 2016, **138**, 14550.

2. ^{1}H, ^{31}P NMR Spectra of the Complexes

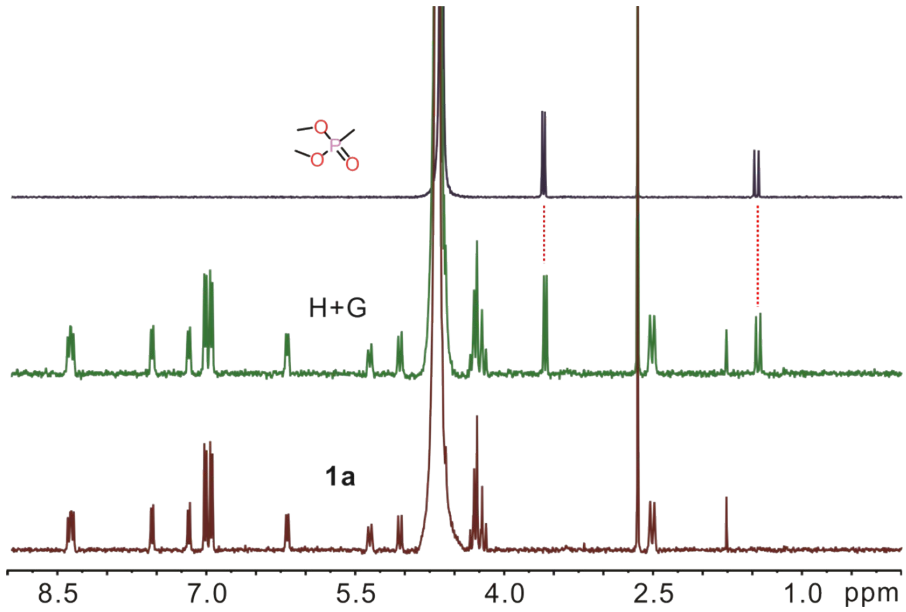

Fig. S1 ^{1}H NMR spectra (400 MHz, D_2O, 2.0×10^{-4} M, 298 K) of (a) Guest **2**, (c) **1a** and (b) their equimolar mixture. The protons of the guest slightly shifted upfield, suggesting the complexation between **2** and **1a**.

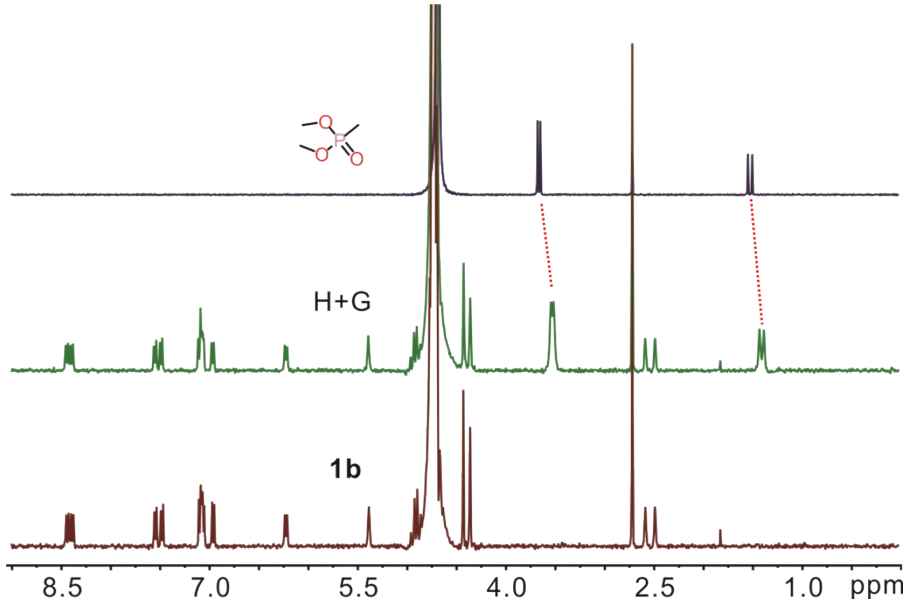

Fig. S2 ^{1}H NMR spectra (400 MHz, D_2O, 2.0×10^{-4} M, 298 K) of (a) Guest **2**, (c) **1b** and (b) their equimolar mixture. The protons of guest shifted upfield and became broadened, suggesting the complexation between **2** and **1b**.

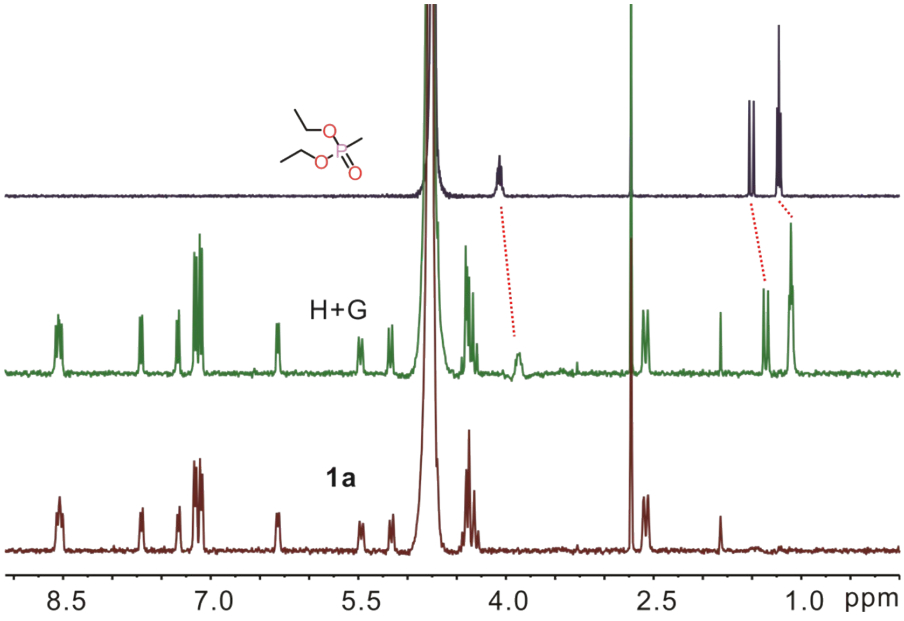

Fig. S3 ^{1}H NMR spectra (400 MHz, D_2O, 2.0×10^{-4} M, 298 K) of (a) Guest **3**, (c) **1a** and (b) their equimolar mixture. In the host-guest mixture, the protons of the guest shifted upfield and became broadened, suggesting the complexation between **3** and **1a**.

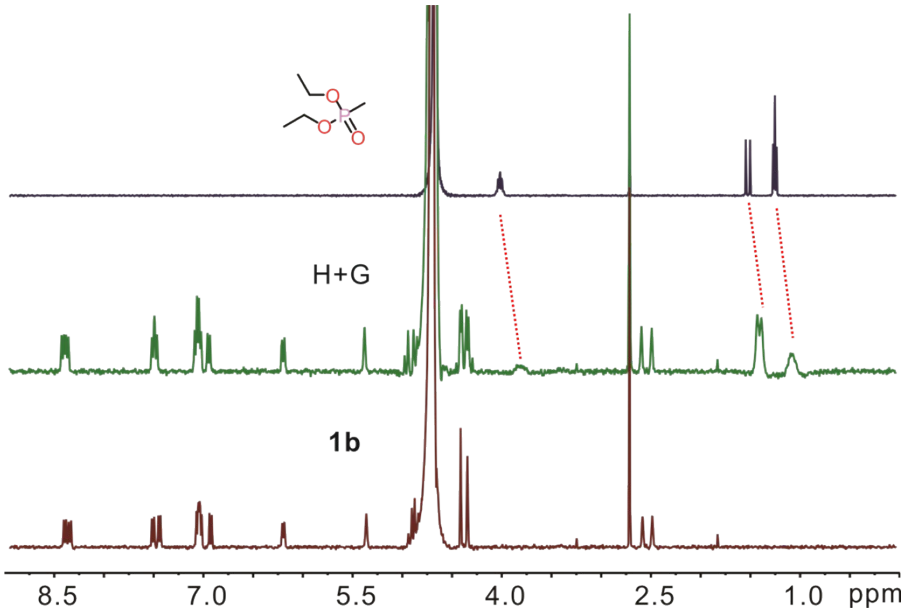

Fig. S4 ^{1}H NMR spectra (400 MHz, D_2O, 2.0×10^{-4} M, 298 K) of (a) Guest **3**, (c) **1b** and (b) their equimolar mixture. In the host-guest mixture, the protons of the guest shifted upfield and became broadened, suggesting the complexation between **3** and **1b**.

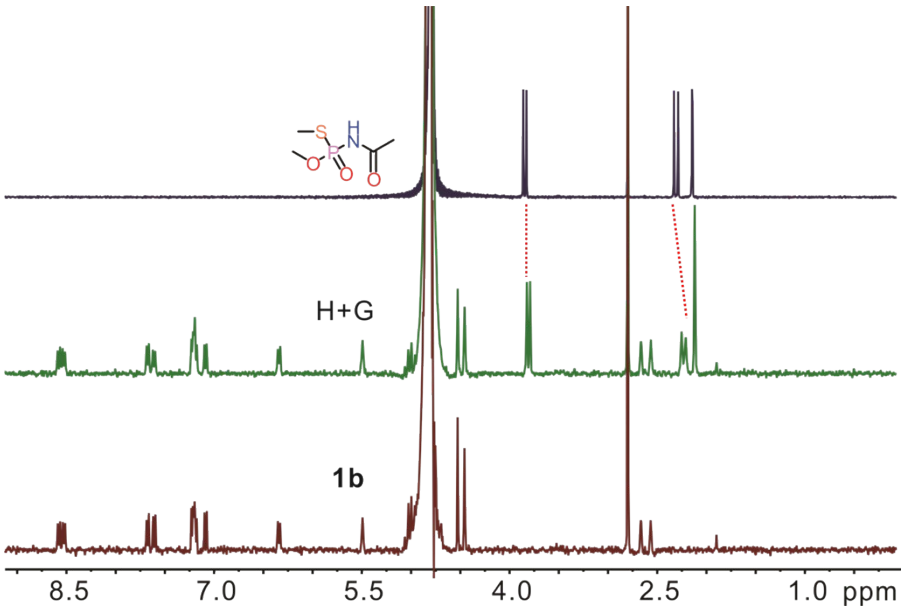

Fig. S5 ^{1}H NMR spectra (400 MHz, D_2O, 2.0×10^{-4} M, 298 K) of (a) Guest **4** (c) **1b** and (b) their equimolar mixture. In the host-guest mixture, the protons of the guest shifted upfield, suggesting the complexation between **4** and **1b**.

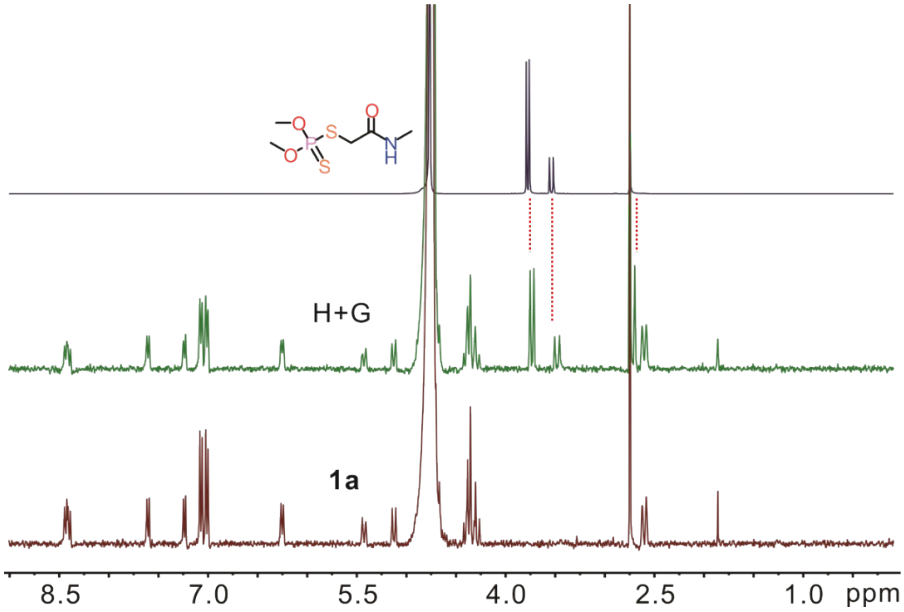

Fig. S6 ^{1}H NMR spectra (400 MHz, D_2O, 2.0×10^{-4} M, 298 K) of (a) Guest **5**, (c) **1a** and (b) their equimolar mixture. In the host-guest mixture, the protons of the guest slightly shifted upfield, suggesting the complexation between **5** and **1a**.

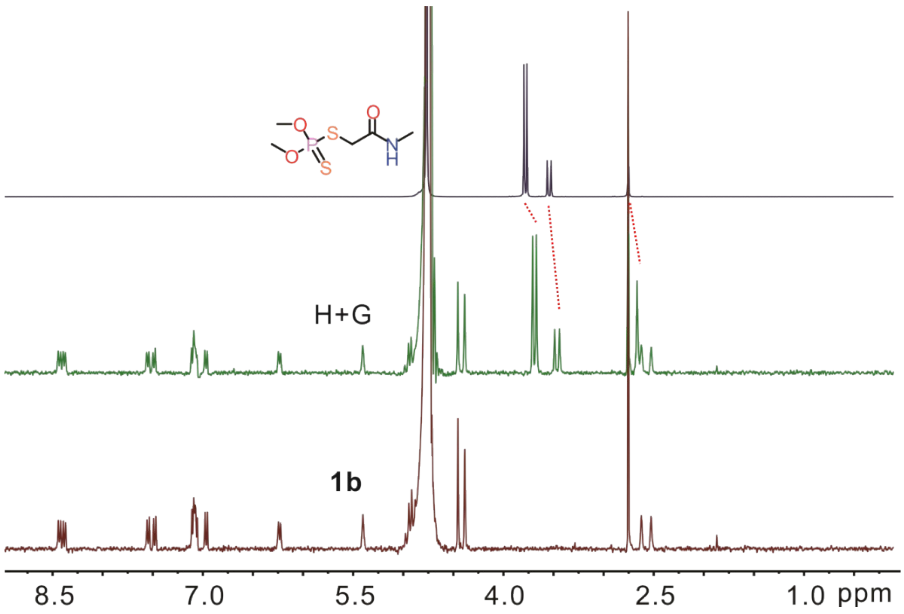

Fig. S7 ^{1}H NMR spectra (400 MHz, D_2O, 2.0×10^{-4} M, 298 K) of (a) Guest **5**, (c) **1b** and (b) their equimolar mixture. In the host-guest mixture, the protons of the guest shifted upfield, suggesting the complexation between **5** and **1b**.

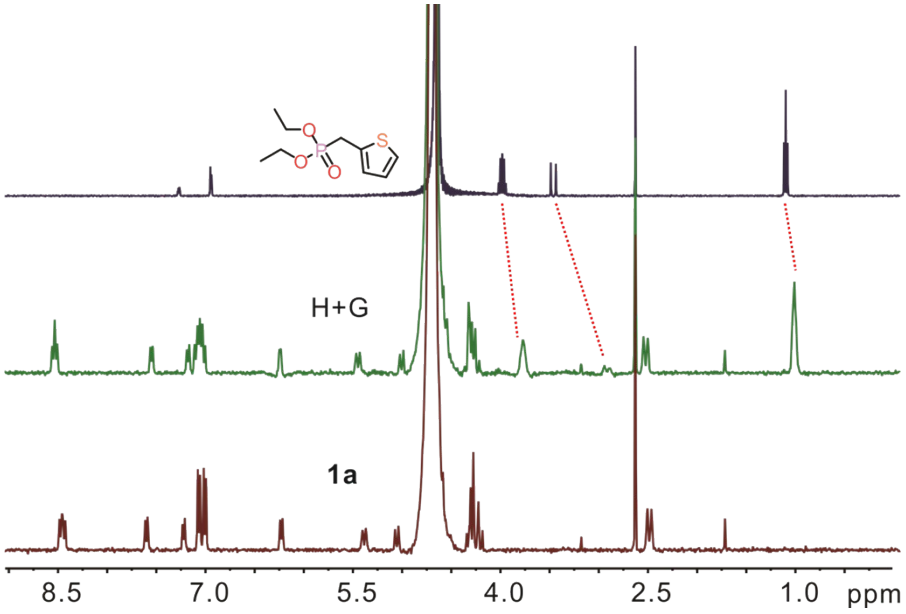

Fig. S8 ^{1}H NMR spectra (400 MHz, D_2O, 2.0×10^{-4} M, 298 K) of (a) Guest **6**, (c) **1a** and (b) their equimolar mixture. In the host-guest mixture, the protons of the guest shifted upfield and become broaden, suggesting the formation of the complex between **6** and **1a**.

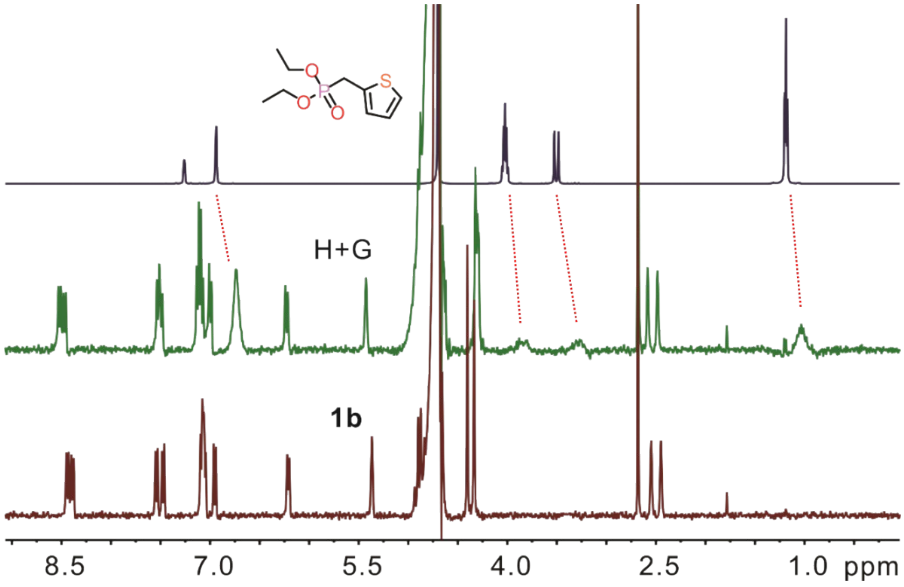

Fig. S9 ^{1}H NMR spectra (400 MHz, D_2O, 2.0×10^{-4} M, 298 K) of (a) Guest **6**, (c)**1b**, and (b) their equimolar mixture. In the host-guest mixture, the protons of the guest shifted upfield and become broaden, suggesting the formation of the complex between **6** and **1b**.

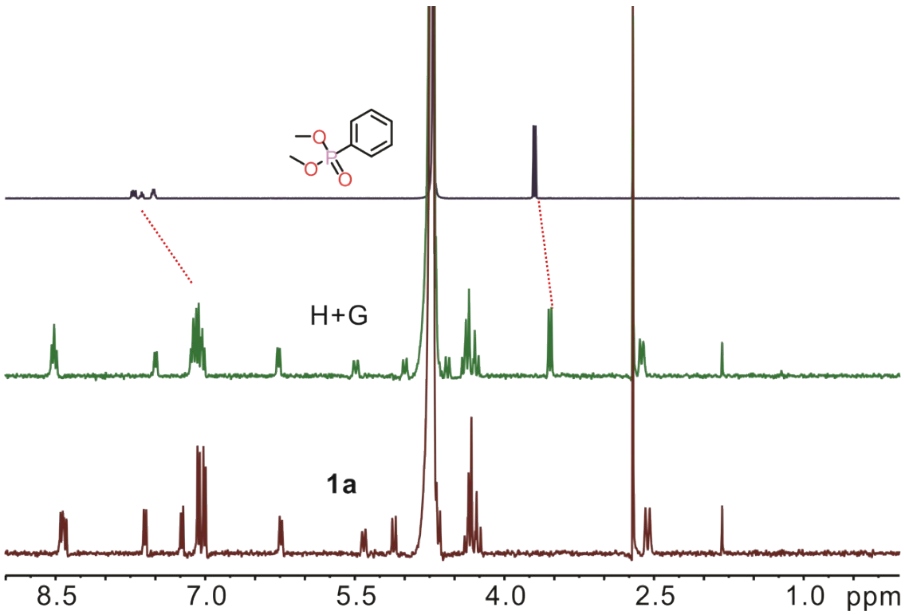

Fig. S10 ^{1}H NMR spectra (400 MHz, D_2O, 2.0×10^{-4} M, 298 K) of (a) Guest **7**, (c) **1a** and (b) their equimolar mixture. In the host-guest mixture, the protons of the guest shifted upfield and become broaden, suggesting the complexation between **7** and **1a**.

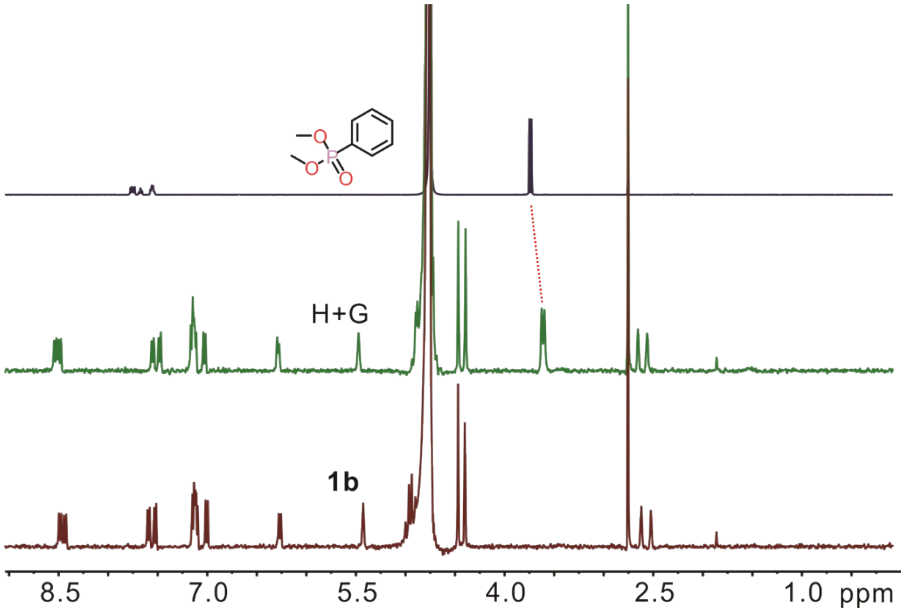

Fig. S11 ^{1}H NMR spectra (400 MHz, D_2O, 2.0×10^{-4} M, 298 K) of (a) Guest **7**, (c) **1b** and (b) their equimolar mixture. In the host-guest mixture, the protons of the guest shifted upfield and become broaden, suggesting the complexation between **7** and **1b**.

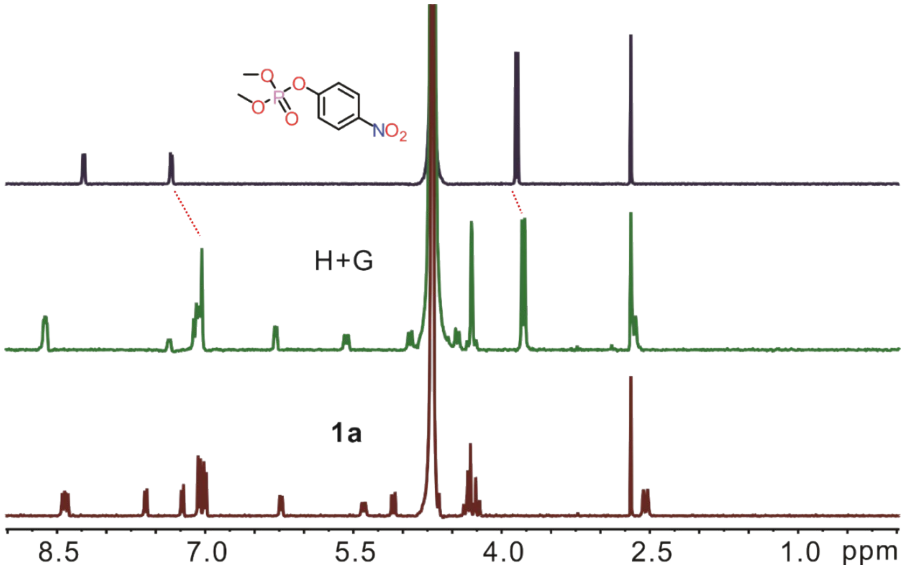

Fig. S12 ^{1}H NMR spectra (400 MHz, D_2O, 2.0×10^{-4} M, 298 K) of (a) Guest **8**, (c) **1a** and (b) their equimolar mixture. In the host-guest mixture, the protons of the guest shifted upfield, and the protons of **1a** largely shifted downfield, suggesting the complexation between **8** and **1a**.

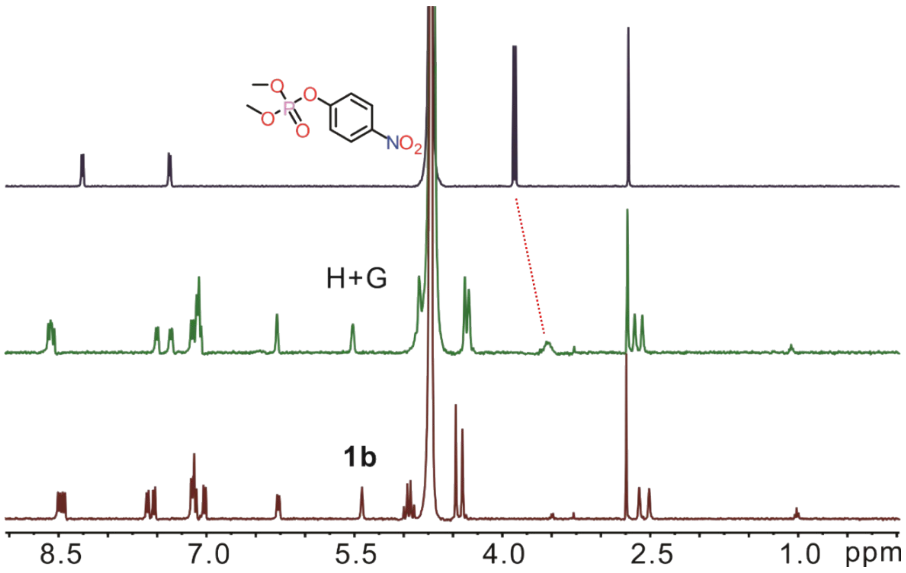

Fig. S13 ^{1}H NMR spectra (400 MHz, D_2O, 2.0×10^{-4} M, 298 K) of (a) Guest **8**, (c) **1b** and (b) their equimolar mixture. The protons of the guest became significantly broadened and rolled into the baseline, while the protons of **1b** shifted downfield, suggesting the complexation between **8** and **1b**.

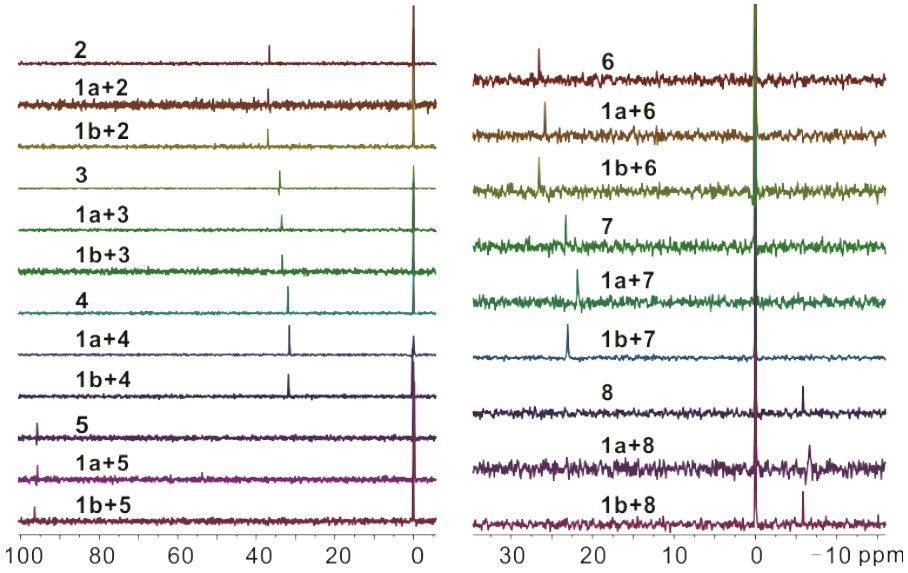

Fig. S14 ^{31}P NMR spectra (162 MHz, D_2O, 5.0×10^{-4} M, 298 K) of Guests **2**-**8** and their equimolar mixture with **1a** and **1b** (with 1.0×10^{-3} M Na_2HPO_4 as the internal standard). When compared to free guests, the shifts of the phosphorus in the complexes were observed, supporting the complex formation.

4. Binding Constants Determined by NMR Titrations

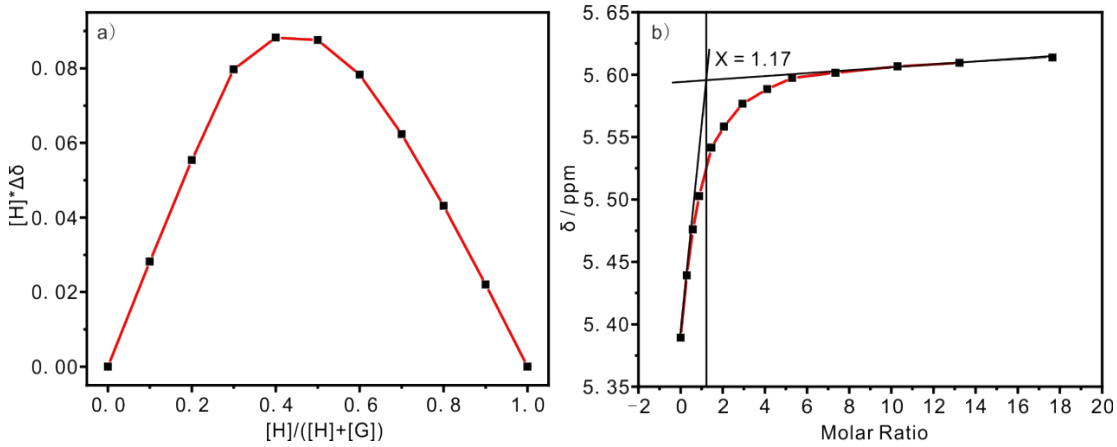

Fig. S15 a) Job's plot obtained by plotting the chemical shift change (*ppm*) of the Host's proton (7+7') in ^{1}H NMR spectra by varying the ratio of the host and the guest against the mole fraction of **1a**. The total concentration of the host and the guest is fixed: [**7**] + [**1a**] = 1.0×10^{-3} M. b) Molar ratio titration plot of **7** and **1a**. These experiments support the 1:1 binding stoichiometry between **7** and **1a** in the 1:1 mixture of D_2O.

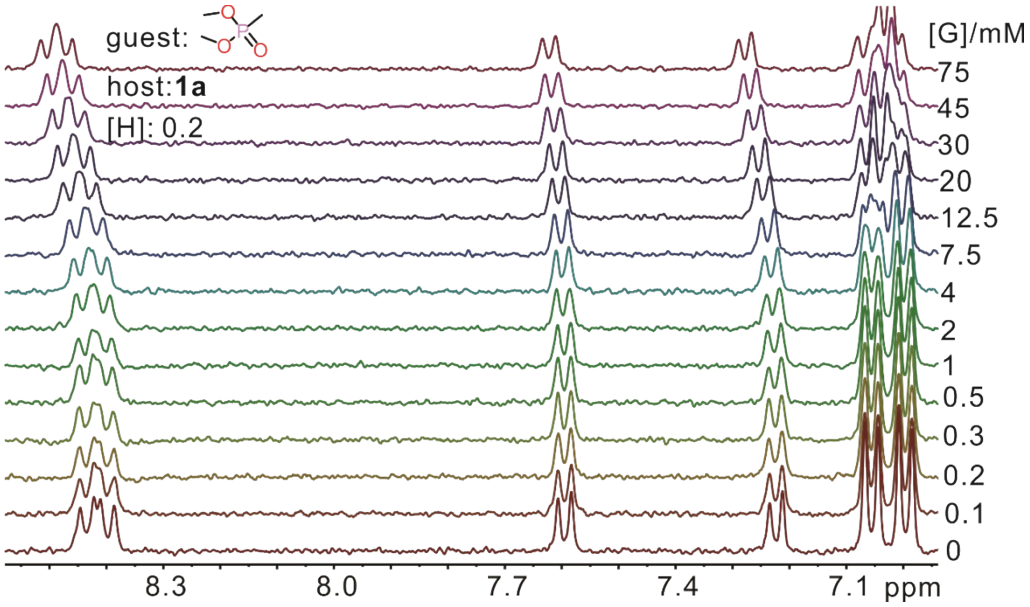

Fig. S16 Partial ^{1}H NMR spectra (400 MHz, D_2O, 298 K) of **1a** (2.0×10^{-4} M) titrated by **2**. From bottom to top, the concentrations of **2** are in the range of $0\sim7.5\times10^{-2}$ M. Protons (1) of **1a** were monitored for the calculation of binding constants. Nonlinear curve-fitting method was then used to obtain the association constant through the following equation by Origin 2018:

$$\delta=\delta_0+\Delta\delta\ (0.5/[H]_0)\ ([G]+[H]_0+1/K-(([G]+[H]_0+1/K)\text{^}2-4[H]_0[G])\text{^}0.5)$$

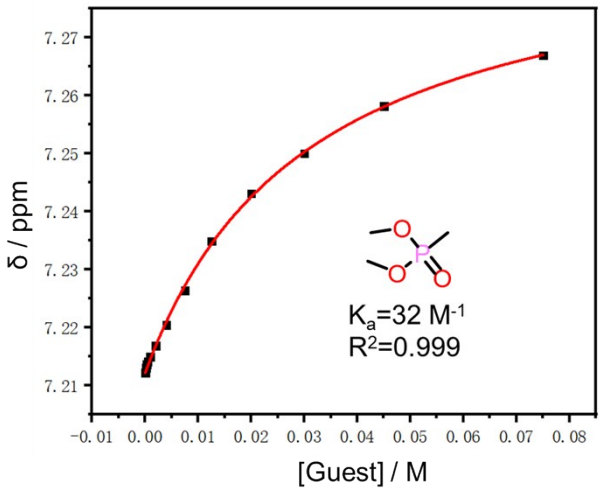

	K_a (M^{-1})	R^2
1st	38	0.996
2nd	32	0.999
3rd	23	0.998
average	31±7	

Fig. S17 Non-linear curve-fitting and association constant for the complexation between **1a** and **2** in D_2O at 298 K.

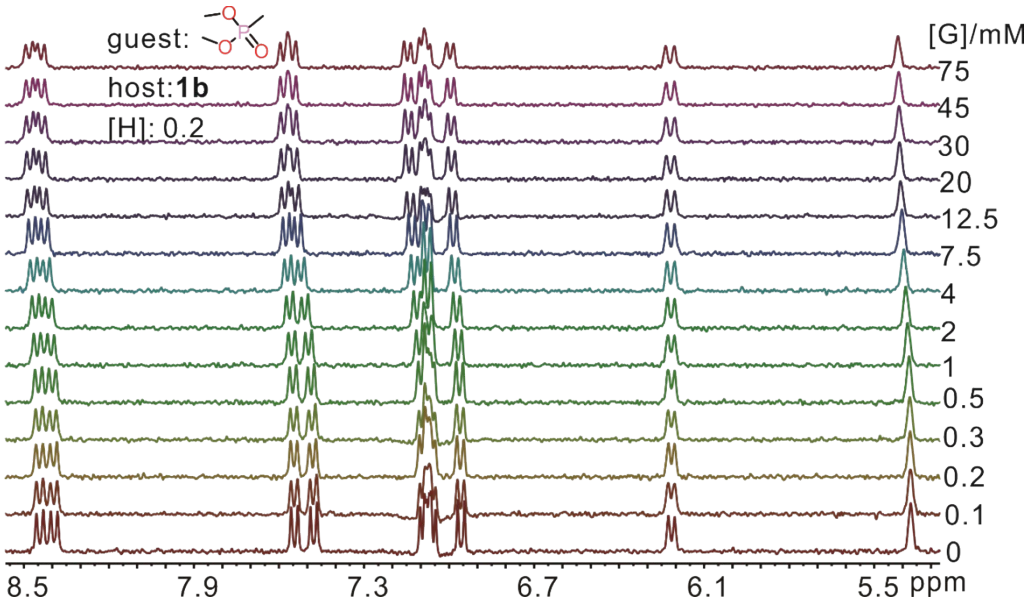

Fig. S18 Partial ^{1}H NMR spectra (400 MHz, D_2O, 298 K) of **1b** (2.0×10^{-4} M) titrated by **2**. From bottom to top, the concentrations of **2** are in the range of 0~7.5×10^{-2} M. Protons (7+7') of **1b** were monitored for the calculation of binding constants.

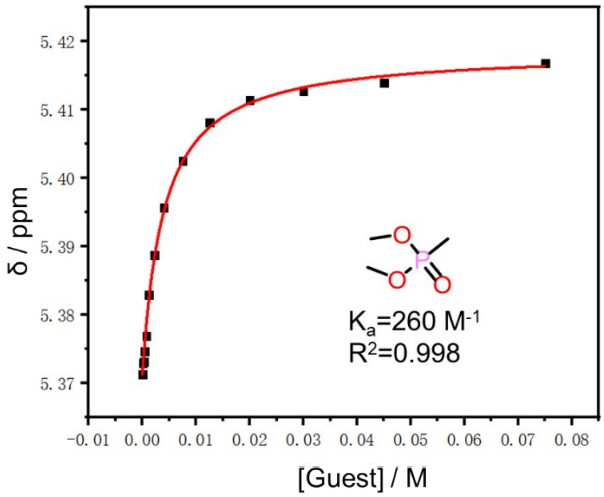

	K_a (M^{-1})	R^2
1st	380	0.990
2nd	260	0.998
3rd	390	0.995
average	340±70	

Fig. S19 Non-linear curve-fitting and association constant for the complexation between **1b** and **2** in D_2O at 298 K.

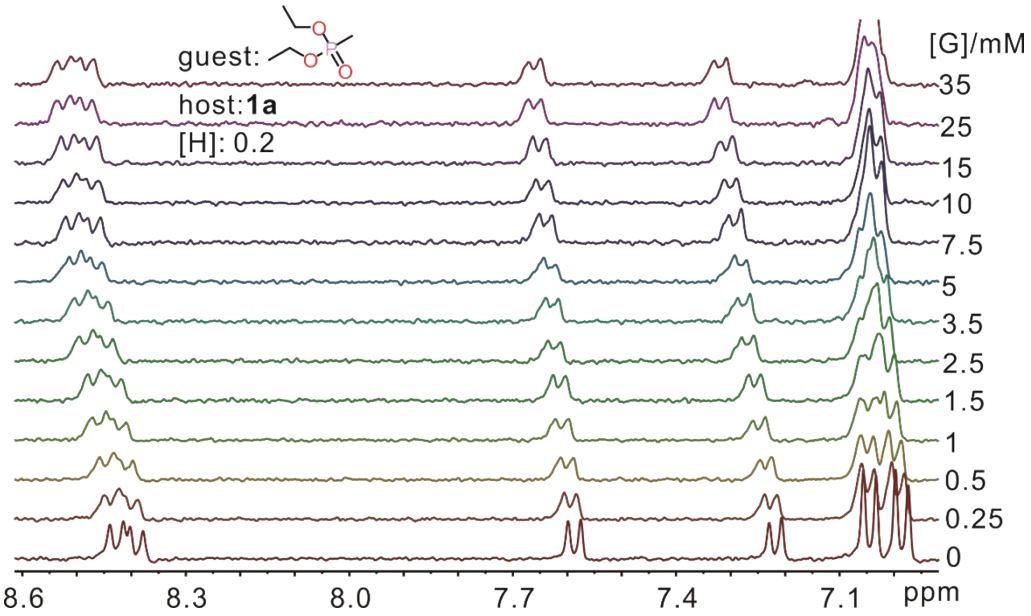

Fig. S20 Partial ^{1}H NMR spectra (400 MHz, D_2O, 298 K) of **1a** (2.0×10^{-4} M) titrated by **3**. From bottom to top, the concentrations of **3** are in the range of 0~3.5×10^{-2} M. Protons (4+4') of **1a** were monitored for the calculation of binding constants.

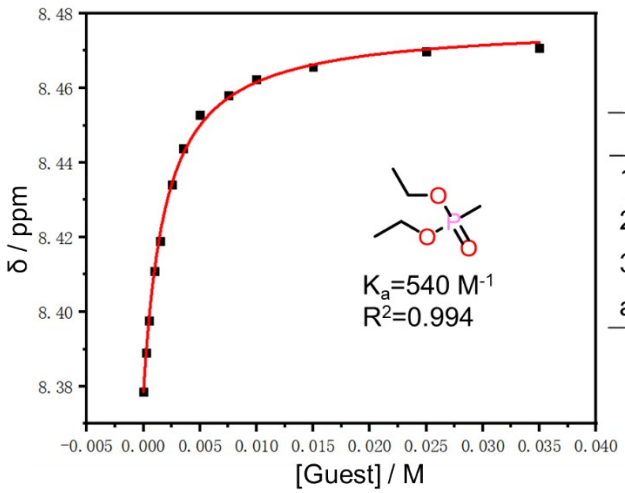

	K_a (M^{-1})	R^2
1st	540	0.994
2nd	540	0.994
3rd	500	0.989
average	530±20	

Fig. S21 Non-linear curve-fitting and association constant for the complexation between **1a** and **3** in D_2O at 298 K.

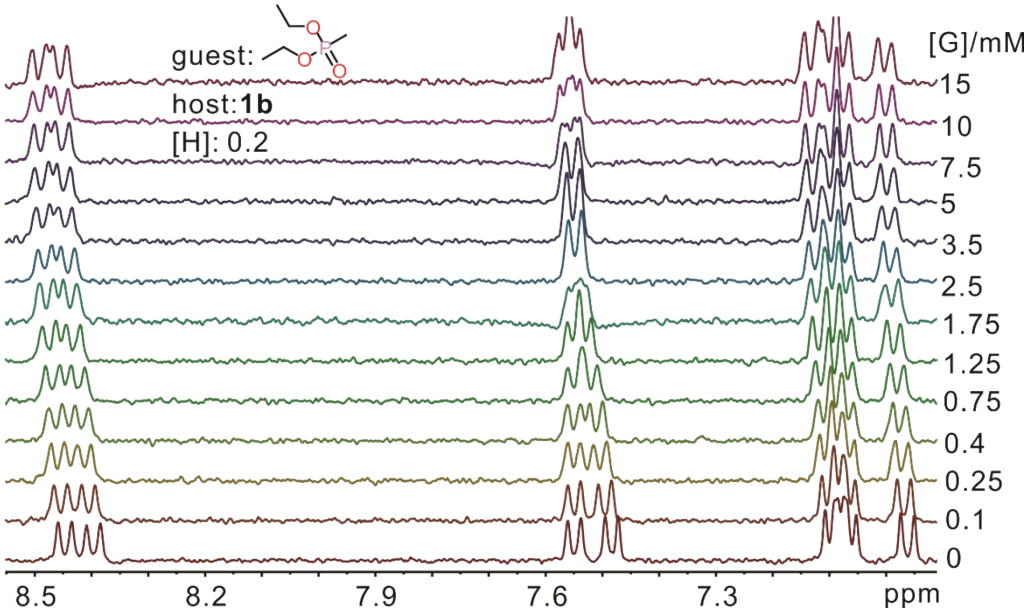

Fig. S22 Partial ^{1}H NMR spectra (400 MHz, D_2O, 298 K) of **1b** (2.0×10^{-4} M) titrated by **3**. From bottom to top, the concentrations of **3** are in the range of 0~1.5×10^{-2} M. Protons (4+4') of **1b** were monitored for the calculation of binding constants.

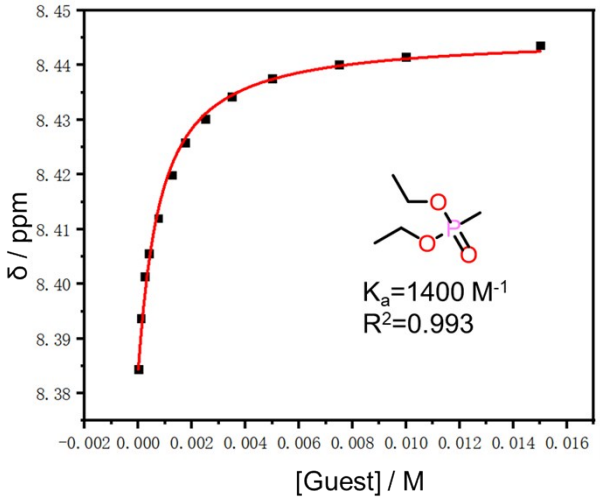

	K_a (M^{-1})	R^2
1st	1500	0.997
2nd	1500	0.994
3rd	1400	0.993
average	1500±60	

Fig. S23 Non-linear curve-fitting and association constant for the complexation between **1b** and **3** in D_2O at 298 K.

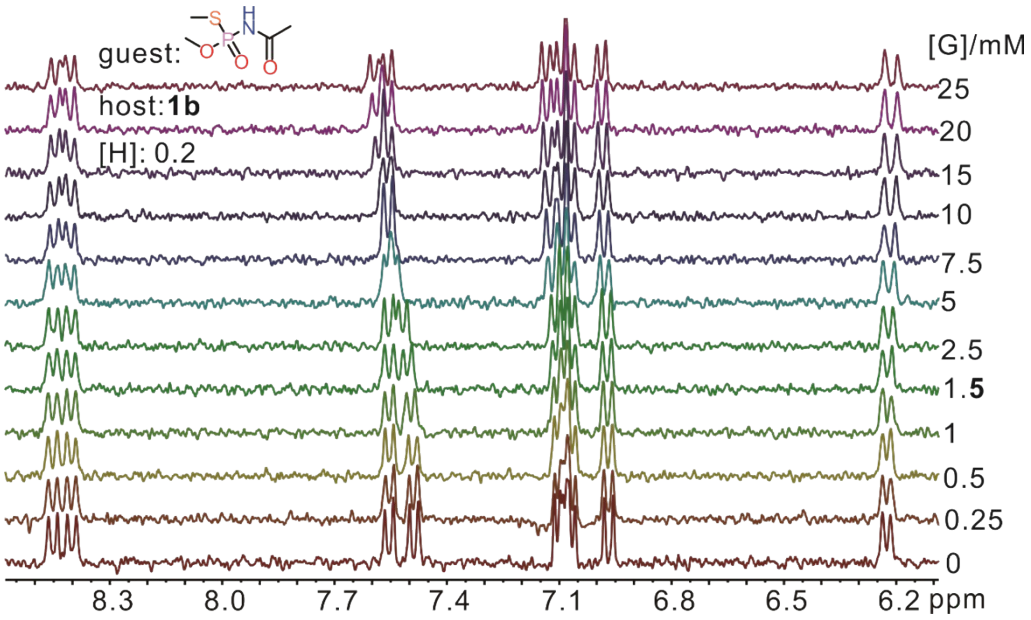

Fig. S24 Partial ^{1}H NMR spectra (400 MHz, D_2O, 298 K) of **1b** (2.0×10^{-4} M) titrated by **4**. From bottom to top, the concentrations of **4** are in the range of 0~2.5×10^{-2} M. Protons (5+5') of **1b** were monitored for the calculation of binding constants.

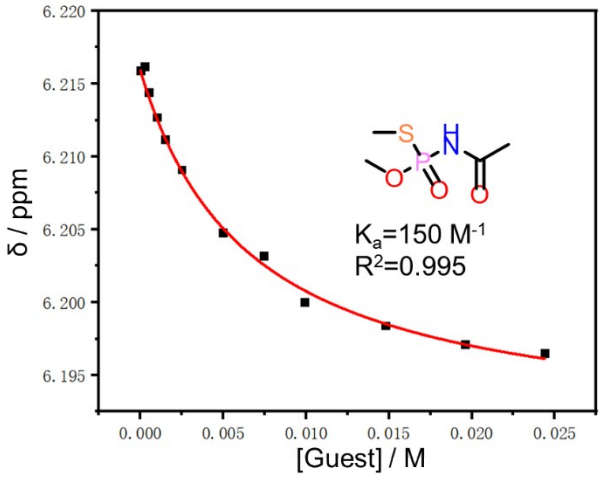

	K_a (M^{-1})	R^2
1st	150	0.995
2nd	110	0.994
3rd	120	0.970
average	130±20	

Fig. S25 Non-linear curve-fitting and association constant for the complexation between **1b** and **4** in D_2O at 298 K.

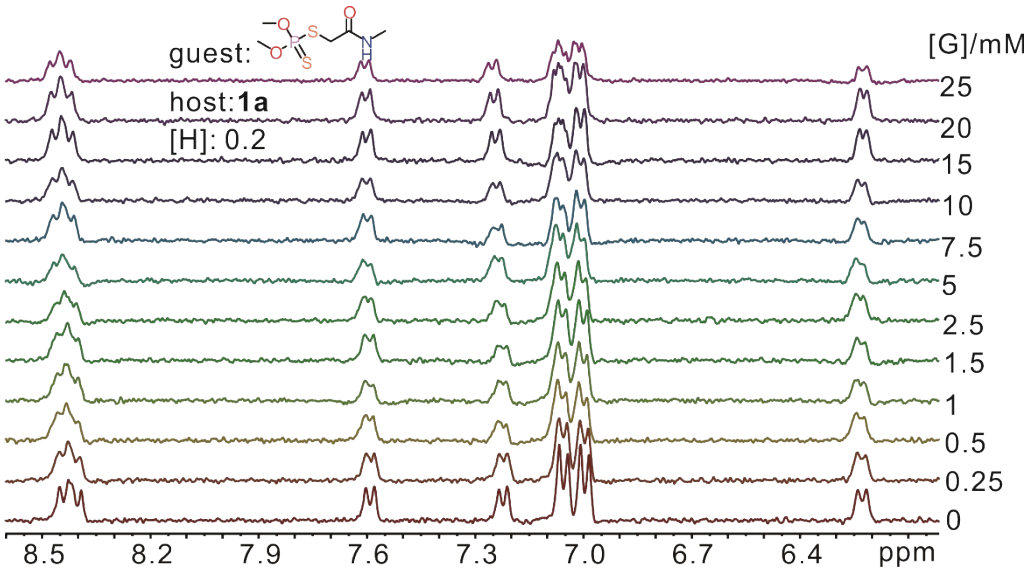

Fig. S26 Partial ^{1}H NMR spectra (400 MHz, D_2O, 298 K) of **1a** (2.0×10^{-4} M) titrated by **5**. From bottom to top, the concentrations of **5** are in the range of 0~2.5×10^{-2} M. Protons (4+4') of **1a** were monitored for the calculation of binding constants.

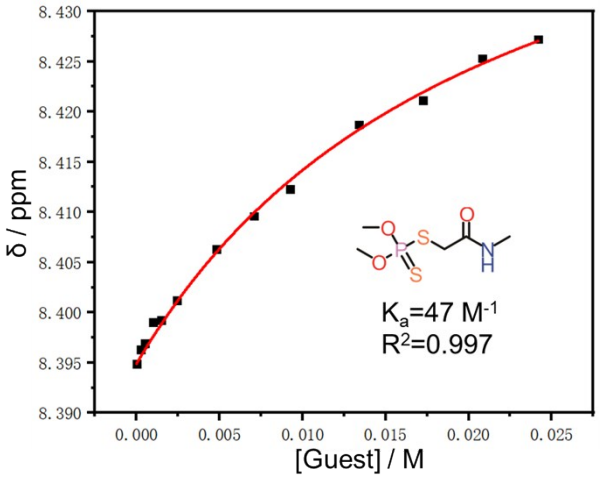

	K_a (M^{-1})	R^2
1st	49	0.991
2nd	47	0.997
3rd	38	0.999
average	45±6	

Fig. S27 Non-linear curve-fitting and association constant for the complexation between **1a** and **5** in D_2O at 298 K.

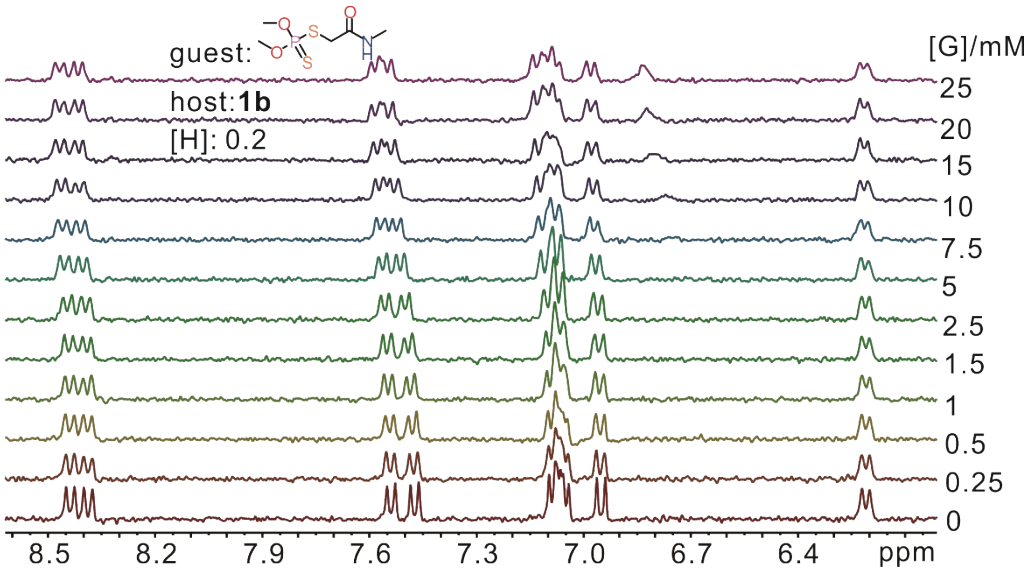

Fig. S28 Partial ^{1}H NMR spectra (400 MHz, D_2O, 298 K) of **1b** (2.0×10^{-4} M) titrated by **5**. From bottom to top, the concentrations of **5** are in the range of $0\sim2.5\times10^{-2}$ M mM. Protons (1+2') of **1b** were monitored for the calculation of binding constants.

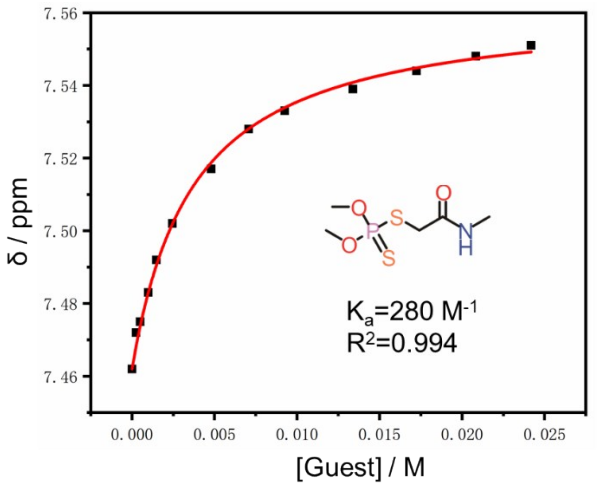

	K_a (M^{-1})	R^2
1st	250	0.997
2nd	280	0.993
3rd	310	0.994
average	280±30	

Fig. S29 Non-linear curve-fitting and association constant for the complexation between **1b** and **5** in D_2O at 298 K.

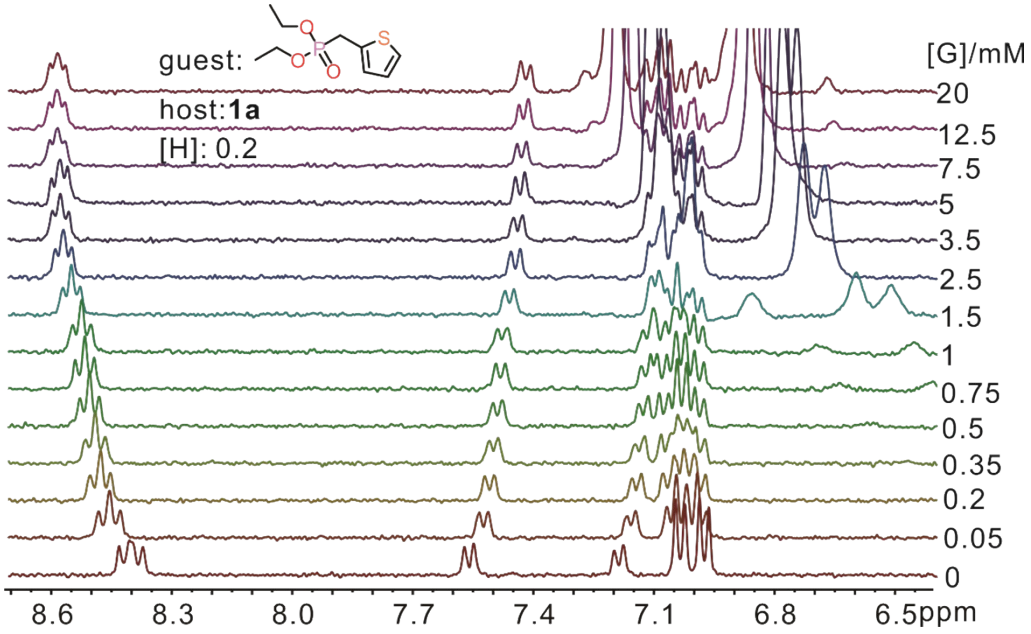

Fig. S30 Partial ^{1}H NMR spectra (400 MHz, D_2O, 298 K) of **1a** (2.0×10^{-4} M) titrated by **6**. From bottom to top, the concentrations of **6** are in the range of 0~2.0×10^{-2} M. Protons (4+4') of **1a** were monitored for the calculation of binding constants. Nonlinear curve-fitting method[i] used here has been reported.

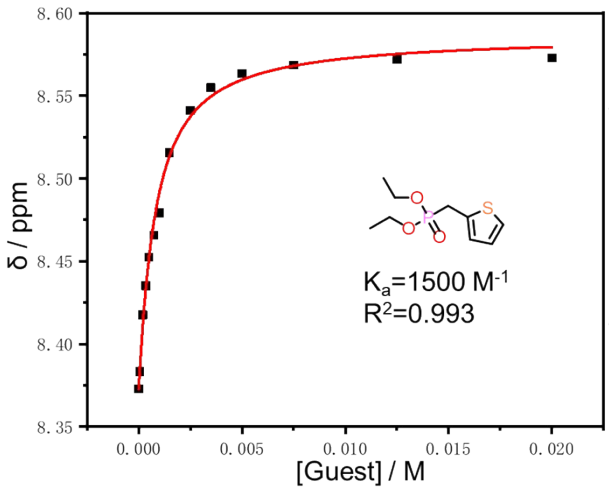

	K_a (M^{-1})	R^2
1st	1300	0.993
2nd	1600	0.993
3rd	1500	0.993
average	1500±200	

Fig. S31 Non-linear curve-fitting and association constant for the complexation between **1a** and **6** in D_2O at 298 K.

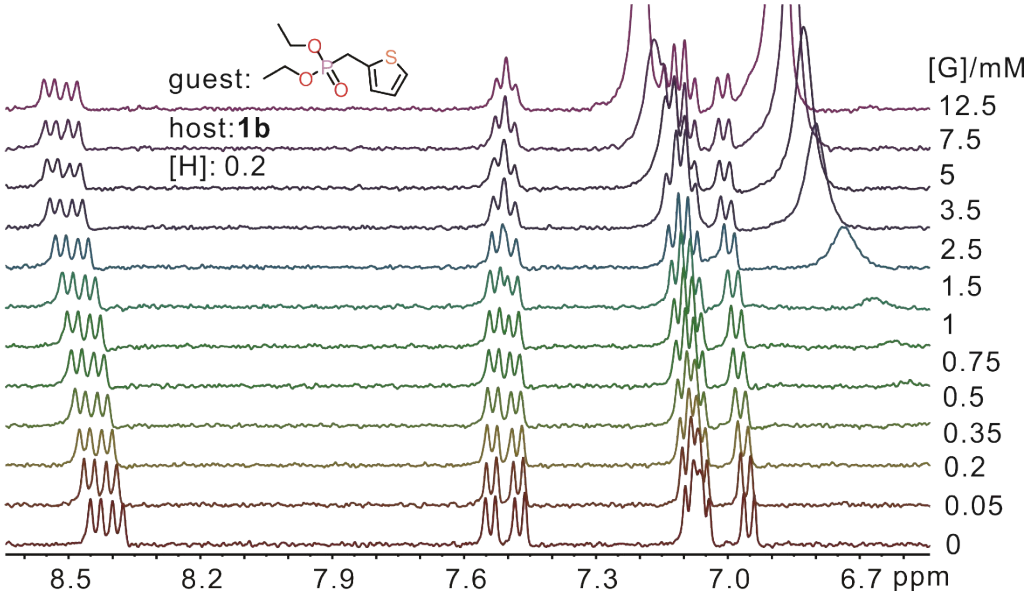

Fig. S32 Partial ^{1}H NMR spectra (400 MHz, D_2O, 298 K) of **1b** (2.0×10^{-4} M) titrated by **6**. From bottom to top, the concentrations of **6** are in the range of 0~1.25×10^{-2} M. Protons (4+4') of **1b** were monitored for the calculation of binding constants.

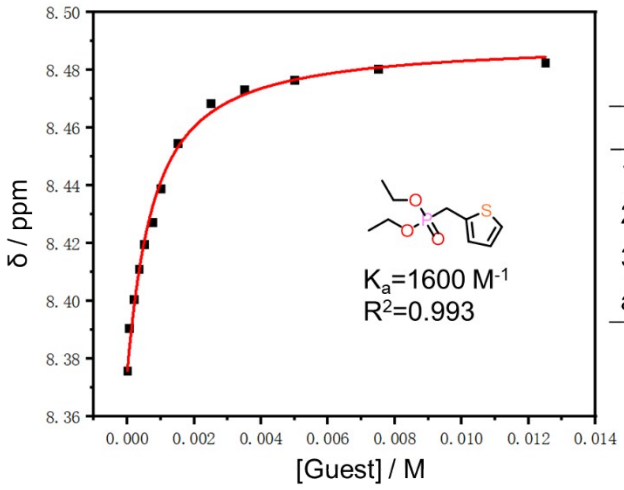

	K_a (M^{-1})	R^2
1st	1600	0.993
2nd	1500	0.989
3rd	1200	0.995
average	1400±200	

Fig. S33 Non-linear curve-fitting and association constant for the complexation between **1b** and **6** in D_2O at 298 K.

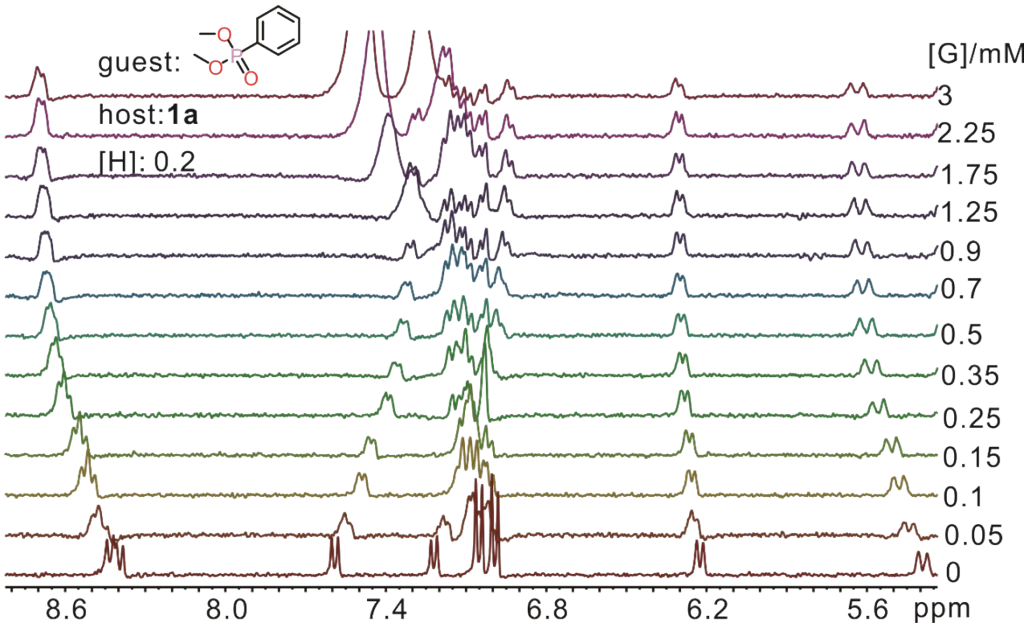

Fig. S34 Partial ^{1}H NMR spectra (400 MHz, D_2O, 298 K) of **1a** (2.0×10^{-4} M) titrated by **7**. From bottom to top, the concentrations of **7** are in the range of 0~3.0×10^{-3} M. Protons (7+7') of **1a** were monitored for the calculation of binding constants.

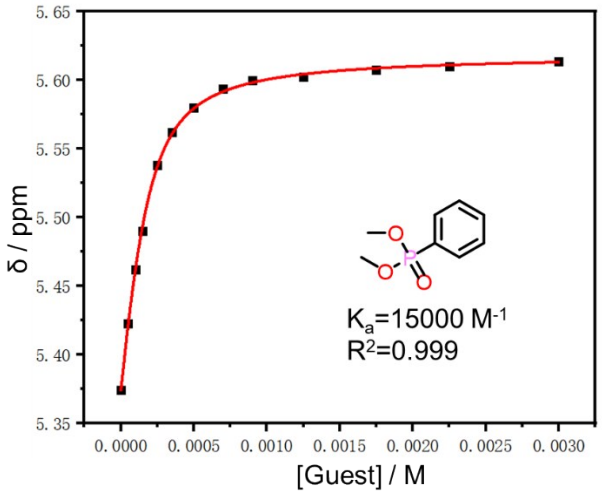

	K_a (M^{-1})	R^2
1st	14000	0.997
2nd	15000	0.998
3rd	15000	0.999
average	15000±600	

Fig. S35 Non-linear curve-fitting and association constant for the complexation between **1a** and **7** in D_2O at 298 K.

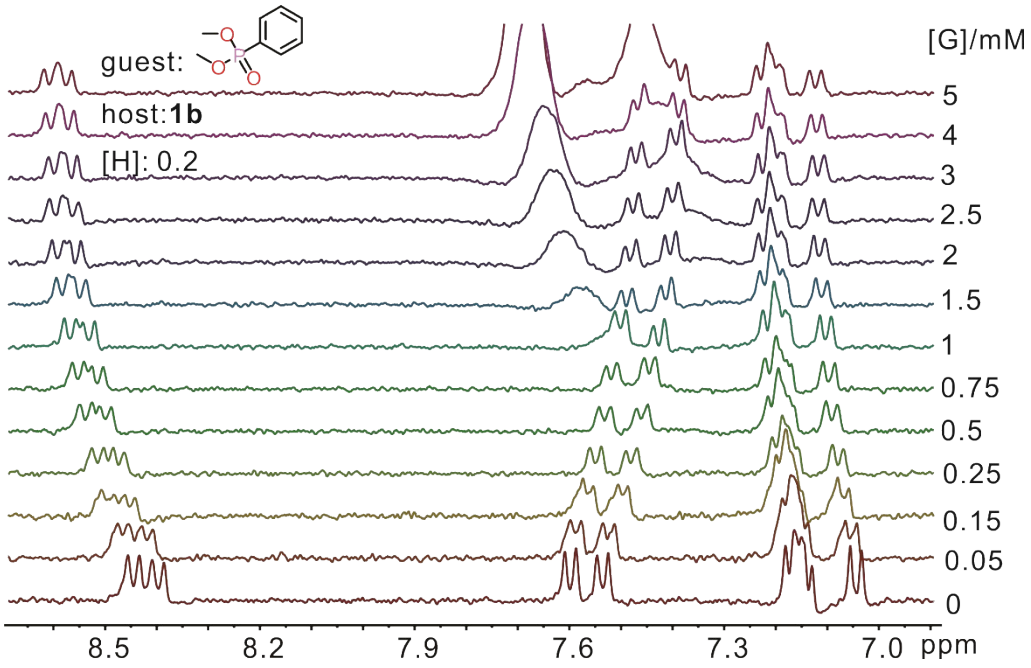

Fig. S36 Partial ^{1}H NMR spectra (400 MHz, D_2O, 298 K) of **1b** (2.0×10^{-4} M) titrated by **7**. From bottom to top, the concentrations of **7** are in the range of 0~5.0×10^{-3} M. Protons (4+4') of **1b** were monitored for the calculation of binding constants.

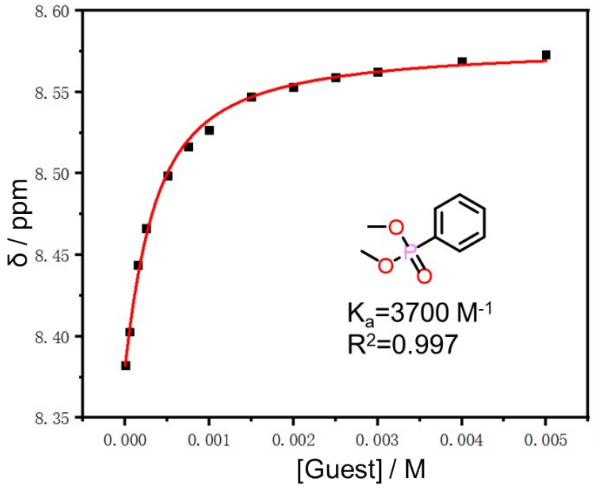

	K_a (M^{-1})	R^2
1st	3500	0.997
2nd	3700	0.997
3rd	4100	0.999
average	3800±300	

Fig. S37 Non-linear curve-fitting and association constant for the complexation between **1b** and **7** in D_2O at 298 K.

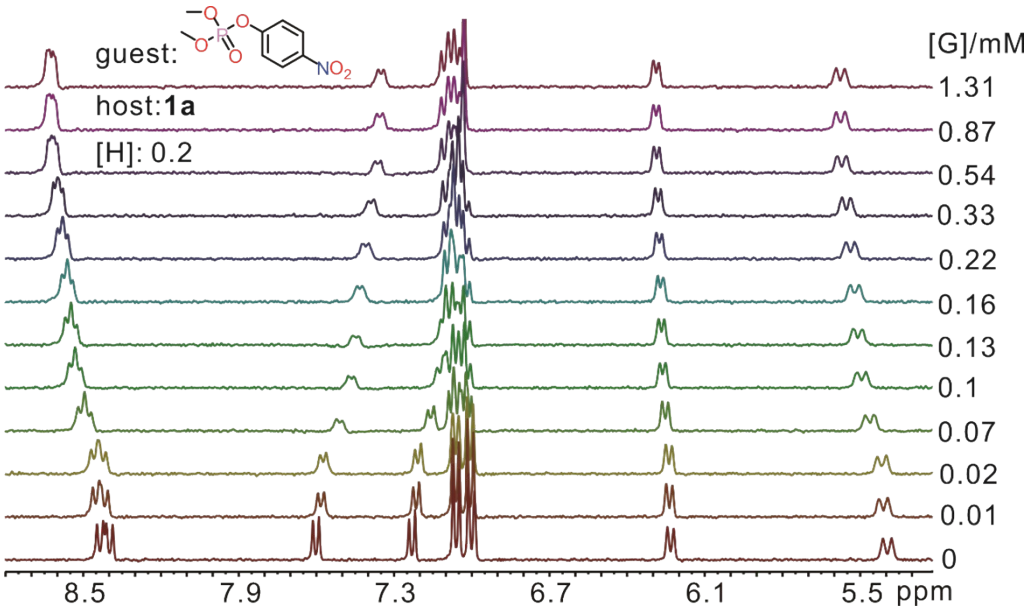

Fig. S38 Partial ^{1}H NMR spectra (400 MHz, D_2O, 298 K) of **1a** (2.0×10^{-4} M) titrated by **8**. From bottom to top, the concentrations of **8** are in the range of 0~1.31×10^{-3} M. Protons (7+7') of **1a** were monitored for the calculation of binding constants.

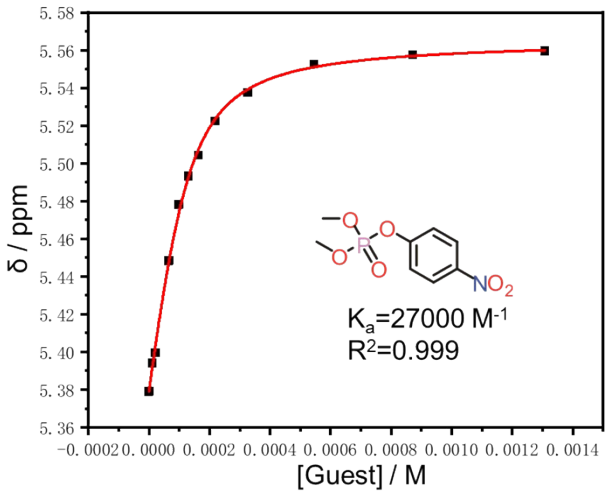

	K_a (M^{-1})	R^2
1st	30000	0.996
2nd	27000	0.999
3rd	26000	0.988
average	28000±2000	

Fig. S39 Non-linear curve-fitting and association constant for the complexation between **1a** and **8** in D_2O at 298 K.

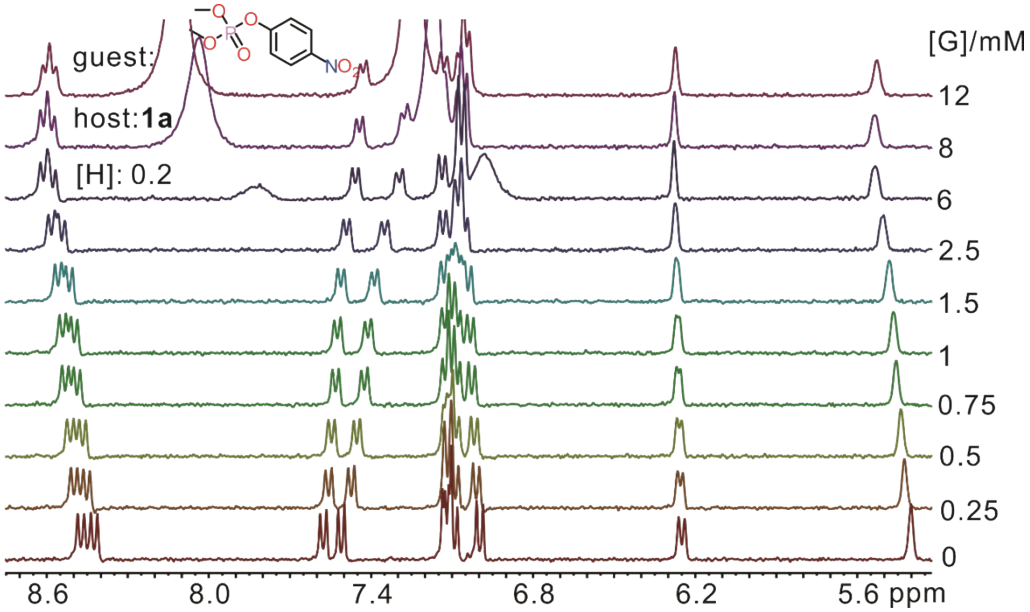

Fig. S40 Partial ^{1}H NMR spectra (400 MHz, D_2O, 298 K) of **1b** (2.0×10^{-4} M) titrated by **8**. From bottom to top, the concentrations of **8** are in the range of 0~1.2×10^{-2} M. Protons (4+4') of **1b** were monitored for the calculation of binding constants.

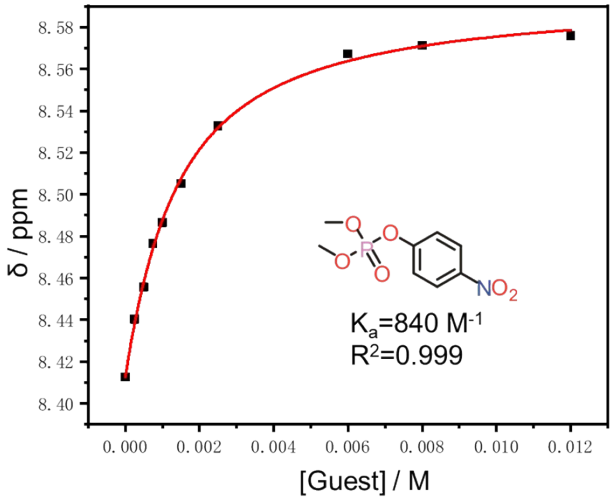

	K_a (M^{-1})	R^2
1st	870	0.979
2nd	840	0.999
3rd	860	0.984
average	860±20	

Fig. S41 Non-linear curve-fitting and association constant for the complexation between **1b** and **8** in D_2O at 298 K.

4. 9:1 H_2O/D_2O Titration Experiments

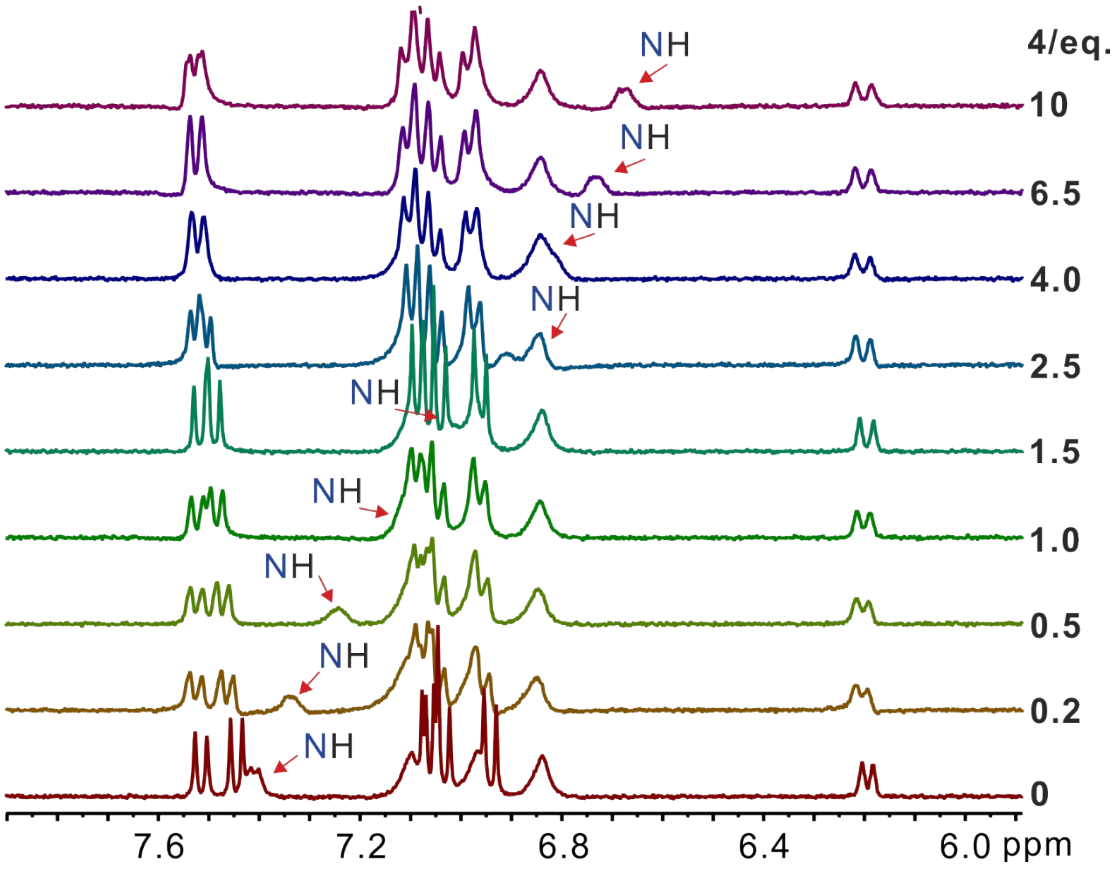

Fig. S42 ^{1}H NMR spectra of **1b** titrated by **3** in H_2O/D_2O (9:1). The water peak was suppressed. The amide protons shift upfield, indicating the hydrogen bonds are weaker between the oxygen atoms of **3** and the amide protons of **1b** than those between 1b and the encapsulated water in its free state.[2]

2 H. Yao, H. Ke, X. Zhang, S. J. Pan, M. S. Li, L. P. Yang, G. Schreckenbach and W. Jiang, *J. Am. Chem. Soc.*, 2018, **140**, 13466.

5. Fluorescence Titration Experiments

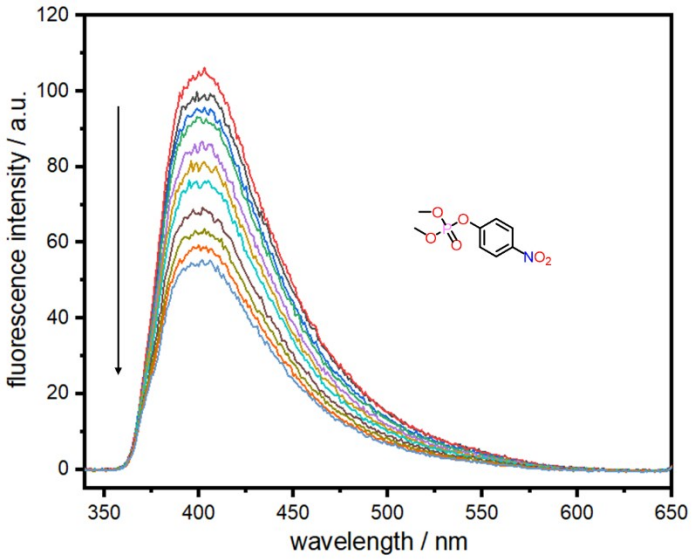

Fig. S43 Fluorescence spectra of **1a** (1.0×10^{-5} M) when titrated with **8** (0~2.1×10^{-5} M) in deionized H_2O at 25 °C

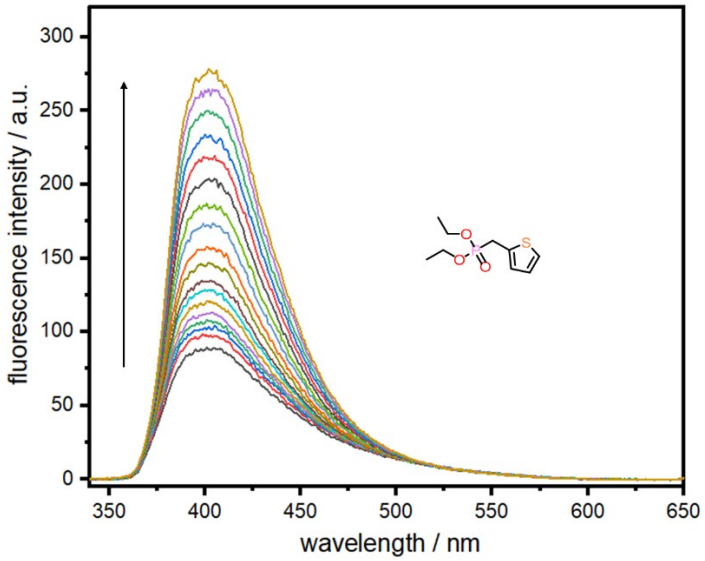

Fig. S44 Fluorescence spectra of **1a** (1.0×10^{-5} M) when titrated with **6** (0~4.1×10^{-4} M) in deionized H_2O at 25 °C

6. In vitro Enzymatic Experiments

The general method was reported by Ellman and co-workers.[3] The principle of this experiment is shown in Fig. S45. Acetylcholinesterase (AChE) can largely increase the hydrolysis speed of Acetylthiocholine-iodide (AICI). The hydrolysed product of AICI can generate a yellow product that have an absorption at 412 nm by reacting with 5,5'-Dithiobis(2-nitrobenzoic acid) (DTNB). Thus, we can monitor the activity of AChE by using UV-vis spectrometer.

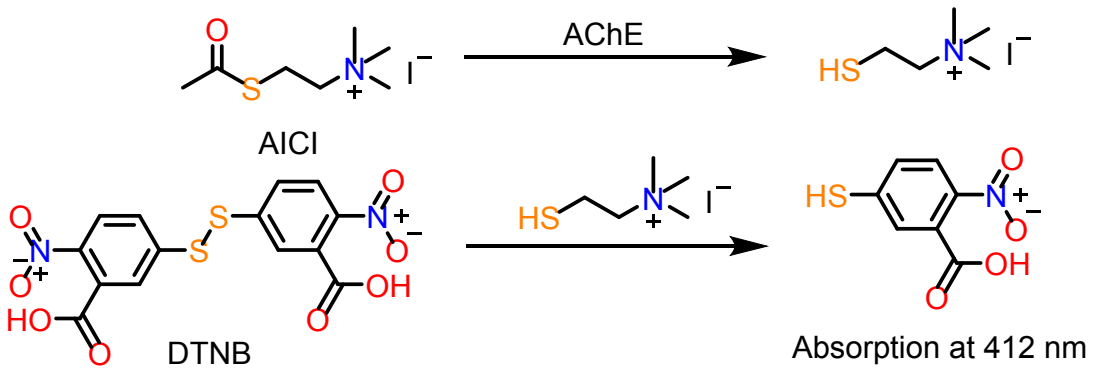

Fig. S45 Mechanism of the Enzyme-based biomimetic experiments by substrate AICI and indicator DTNB.

AChE (200 u/g), substrate AICI, and indicator DTNB are all commercially available. 15 mM DTNB solution, 15 mM AICI solution and 0.85 u/mL AChE solution was prepared in PBS buffer (10 mM, pH = 7.2). Before the experiment, 2.65 mL PBS buffer, 50 μL AChE (4.25×10^{-2} u) and 100 μL DTNB (1.5×10^{-3} mmol) mixture was preheated under 37 °C for 10 mins. After that, 50 μL AICI (7.5×10^{-4} mmol) was injected to the mixture. The resulting solution was monitored by using UV-vis spectrometer. Molecular tube **1a** and paraoxon were added after preheated and before the injection of AICI.

3 G. L. Ellman, K. D. Courtney, V. Andres Jr. and R. M. Featherstone. *Biochem. Parmacol.*, 1961, **7**, 88.

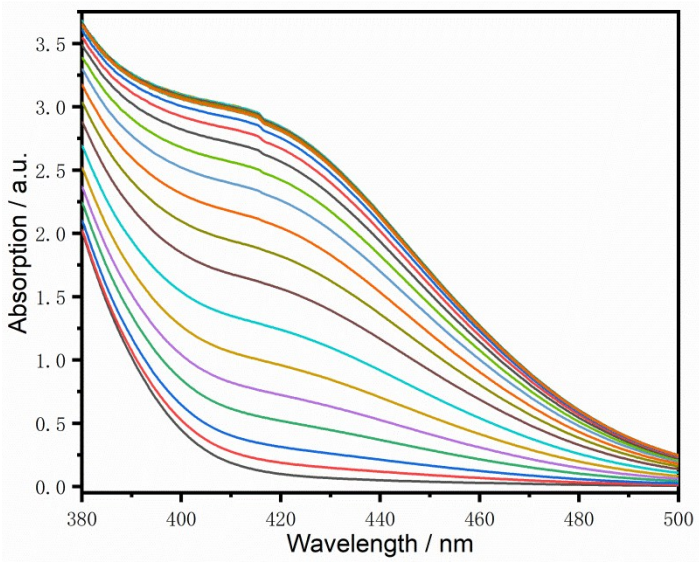

Fig. S46 UV-vis monitoring of enzyme-based experiment at 37 °C with: 4.25×10^{-2} u AChE, 1.5×10^{-3} mmol DTNB and 7.5×10^{-4} mmol AICI.

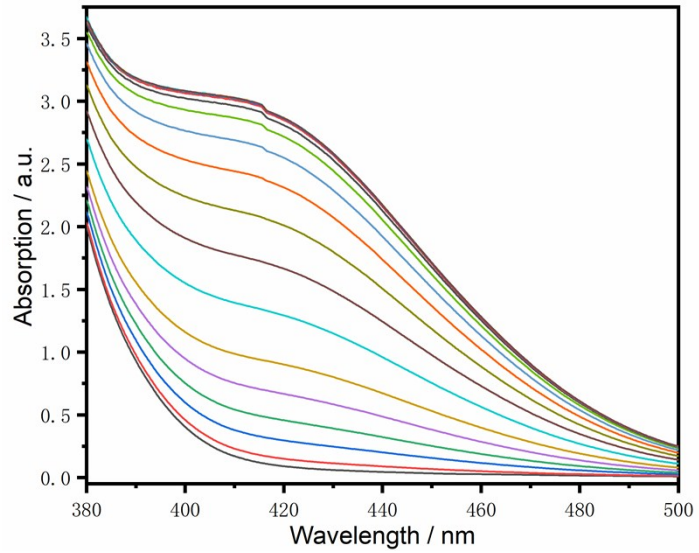

Fig. S47 UV-vis monitoring of enzyme-based experiment at 37 °C with: 7.5×10^{-4} mmol **1a**, 4.25×10^{-2} u AChE, 1.5×10^{-3} mmol DTNB and 7.5×10^{-4} mmol AICI.

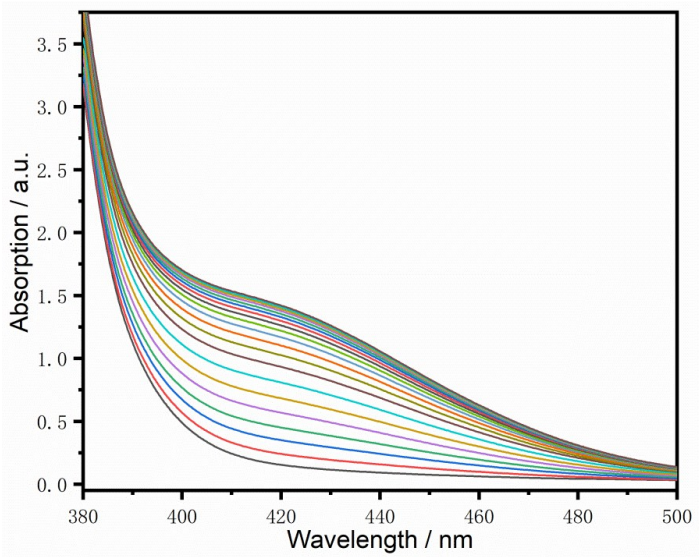

Fig. S48 UV-vis monitoring of enzyme-based experiment at 37 °C with: 3.75×10^{-3} mmol **1a**, 4.25×10^{-2} u AChE, 1.5×10^{-3} mmol DTNB, 7.5×10^{-4} mmol AICI and 7.5×10^{-4} mmol paraoxon.

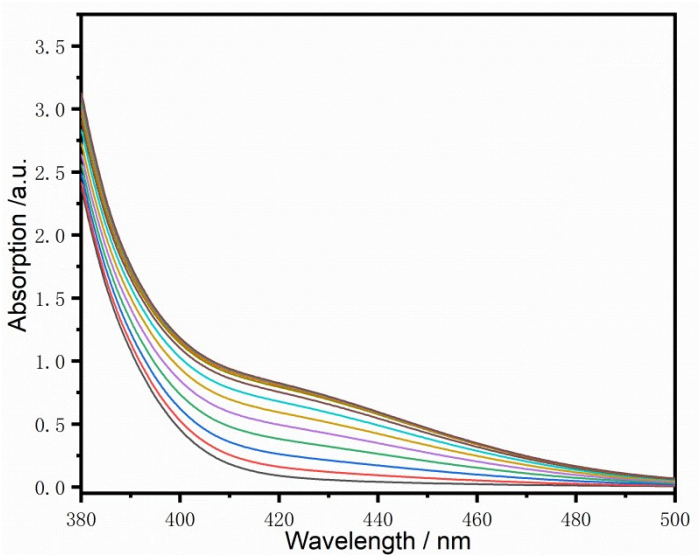

Fig. S49 UV-vis monitoring of enzyme-based experiment at 37 °C with: 7.5×10^{-4} mmol **1a**, 4.25×10^{-2} u AChE, 1.5×10^{-3} mmol DTNB, 7.5×10^{-4} mmol AICI and 7.5×10^{-4} mmol paraoxon.

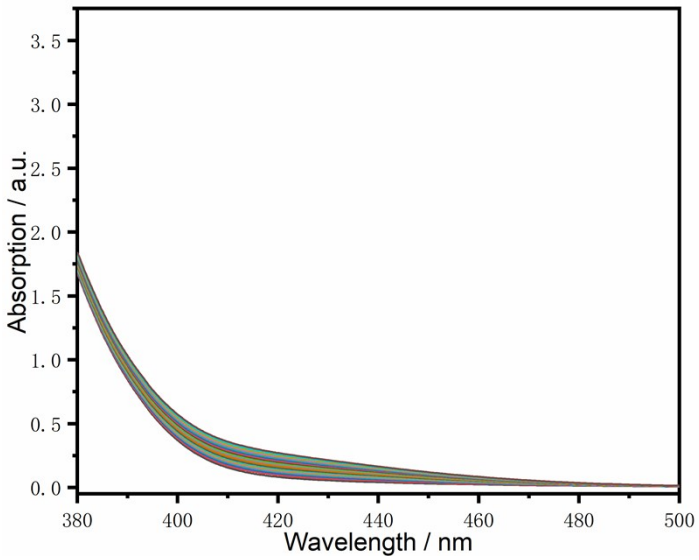

Fig. S50 UV-vis monitoring of enzyme-based experiment at 37°C with: 4.25×10^{-2} u AChE, 1.5×10^{-3} mmol DTNB, 7.5×10^{-4} mmol AICI and 7.5×10^{-4} mmol paraoxon.

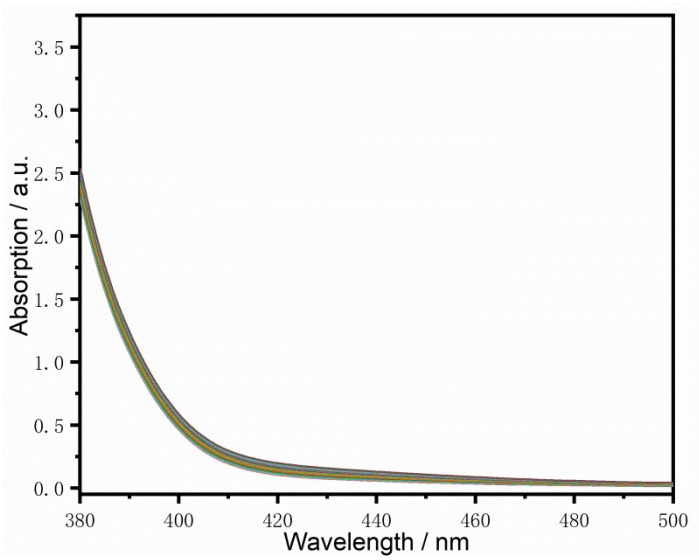

Fig. S51 UV-vis monitoring of enzyme-based experiment at 37 °C with: 7.5×10^{-4} mmol **1a**, 1.5×10^{-3} mmol DTNB and 7.5×10^{-4} mmol AICI.

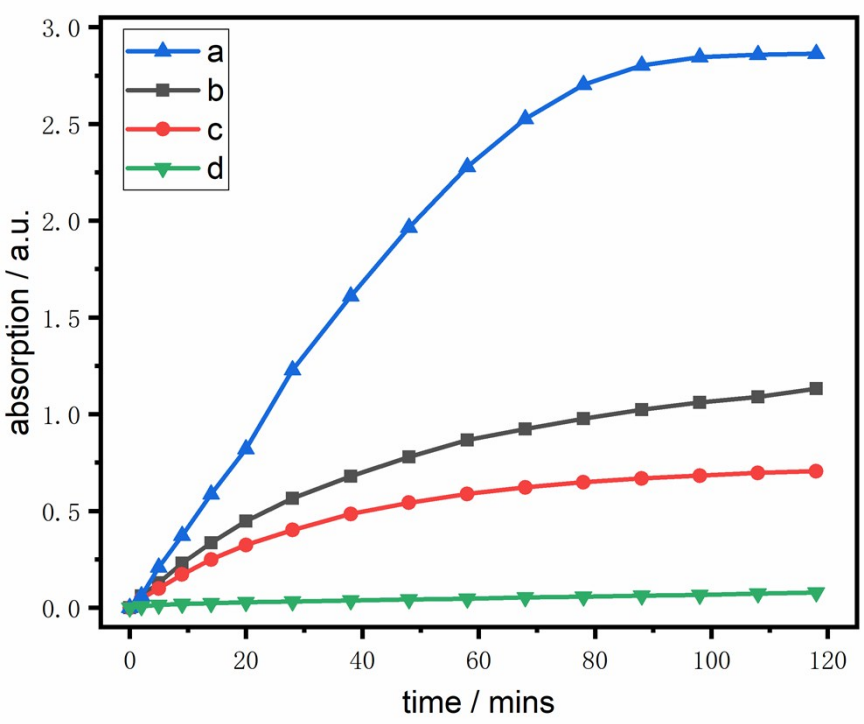

Fig. S52 Biomimetic enzyme-based experiments (37 °C, UV-vis absorption at 412nm) for the prevention of paraoxon's toxicity to acetylcholinesterase (AChE) using molecular tube **1a**. a) AChE + substrate + indicator; b) AChE + substrate + indicator + 1 eq. paraoxon + 5 eq. **1a** (after 30 s); c) AChE + substrate + indicator + 1 eq. paraoxon + 5 eq. **1a** (after 60 s); d) AChE + substrate + indicator + 1 eq. paraoxon;

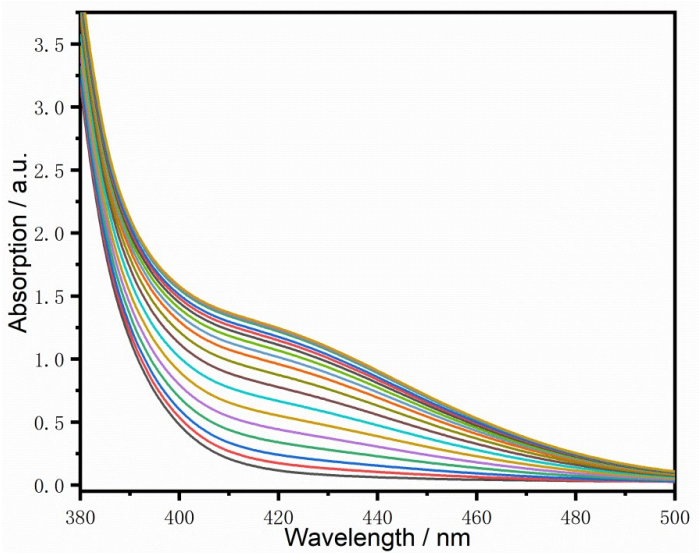

Fig. S53 UV-vis monitoring of enzyme-based experiment at 37 °C with: 4.25×10^{-2} u AChE, 1.5×10^{-3} mmol DTNB, 7.5×10^{-4} mmol AICI and 7.5×10^{-4} mmol paraoxon. 3.75×10^{-3} mmol **1a** was added 30 s after the injected of paraoxon.

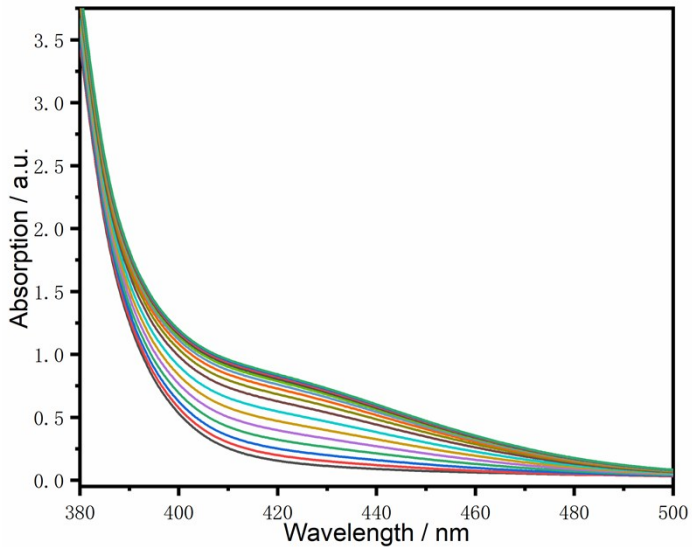

Fig. S54 UV-vis monitoring of enzyme-based experiment at 37 °C with: 4.25×10^{-2} u AChE, 1.5×10^{-3} mmol DTNB, 7.5×10^{-4} mmol AICI and 7.5×10^{-4} mmol paraoxon. 3.75×10^{-3} mmol **1a** was added 60 s after the injected of paraoxon.

7. Binding between AICI and 1a

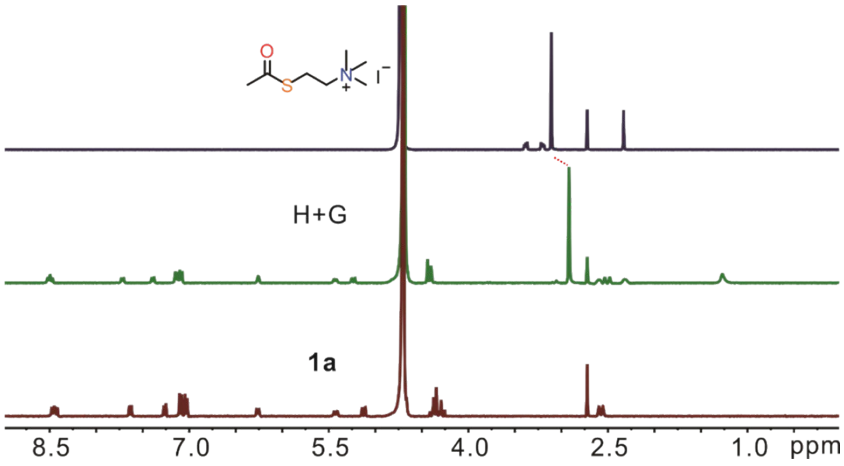

Fig. S55 ^{1}H NMR spectra (400 MHz, D_2O, 4.0×10^{-4} M, 298 K) of (a) Guest **AICI**, (c) **1a** and (b) their equimolar mixture. In the host-guest mixture, the protons of the guest shifted upfield, suggesting the complexation between **AICI** and **1a**.

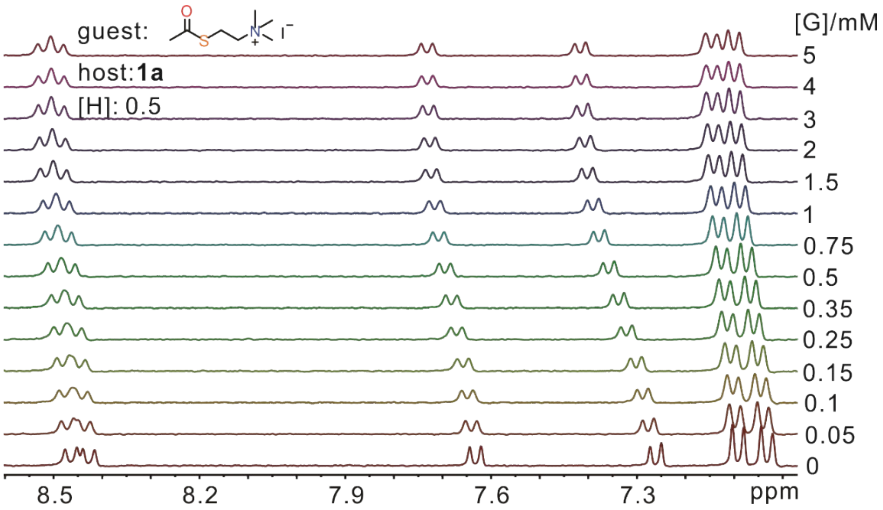

Fig. S56 Partial ^{1}H NMR spectra (400 MHz, D_2O, 298 K) of **1a** (5.0×10^{-4} M) titrated by **AICI**. From bottom to top, the concentrations of **AICI** are in the range of 0~5.0×10^{-3} M. Protons (2') of **1a** were monitored for the calculation of binding constants.

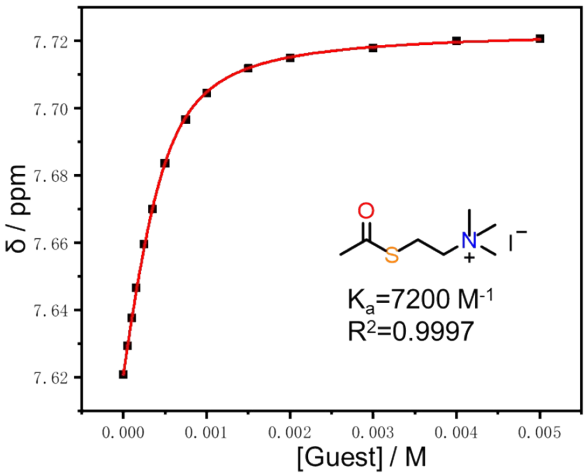

	K_a (M^{-1})	R^2
1st	8000	0.9994
2nd	6600	0.9990
3rd	7200	0.9997
average	7300±700	

Fig. S57 Non-linear curve-fitting and association constant for the complexation between **1a** and **AICI** in D_2O at 298 K.